Progress in Physics of Applied Materials 7 (2027), Serial Number 14, 85-94

Semnan University

Progress in Physics of Applied Materials

journal homepage: https://ppam.semnan.ac.ir/

# Time-Dependent Growth Behavior of Alumina Layers on Aluminum during plasma-Assisted Electrochemical Oxidation in a Plasma–Liquid Interface

**Z. Dehghani** *

*Plasma and Nuclear Fusion Research School, Nuclear Science and Technology Research Institute, Tehran, Iran*

**ARTICLE INFO**

Article history:
Received: 4 June 2026
Revised: 25 July 2026
Accepted: 2 August 2026
Published online: 26 August 2026

Keywords:
Aluminum;
Microplasma;
Plasma–liquid interaction;
Surface modification;
AFM;
SEM.

**ABSTRACT**

Surface modification of aluminum by plasma-assisted electrochemical techniques has attracted considerable interest due to their ability to produce oxide layers with enhanced surface properties. In this study, aluminum surfaces were treated using a DC microplasma-assisted electrochemical process in a 0.05 M NaOH electrolyte under atmospheric-pressure conditions. The effect of treatment duration on oxide-layer development was investigated by varying the processing time from 5 to 20 min while maintaining constant discharge parameters. Surface morphology and roughness were characterized by atomic force microscopy (AFM) and scanning electron microscopy (SEM), and phase composition was analyzed using X-ray diffraction (XRD). AFM results showed that surface roughness increased with treatment time and reached a maximum after 10 min, indicating accelerated oxide growth. Further treatment led to a reduction in roughness, suggesting surface reorganization during prolonged plasma exposure. SEM observations revealed the formation of porous, interconnected needle-like oxide structures on the treated surface. XRD analysis confirmed the formation of crystalline $\gamma$-$Al_2O_3$ after 20 min of treatment. Based on the experimental findings, a three-stage growth mechanism involving oxide nucleation, oxide growth, and plasma-assisted surface reorganization was proposed. The results demonstrate that treatment duration is a key parameter governing the structural evolution of alumina layers formed in plasma–liquid systems and provide insight into the controlled modification of aluminum surfaces by microplasma-assisted electrochemical oxidation.

## 1. Introduction

Aluminum and its alloys have become indispensable engineering materials in modern industries owing to their unique combination of low density, high specific strength, excellent thermal conductivity, and favorable corrosion resistance characteristics [1,2]. These properties have enabled their widespread utilization in aerospace structures, transportation systems, electronics, energy devices, and chemical processing equipment. Nevertheless, despite the spontaneous formation of a thin native oxide film, aluminum surfaces often suffer from insufficient hardness, limited wear resistance, and degradation under aggressive service environments, which can significantly restrict their long-term performance and reliability [3,4]. Consequently, the development of effective surface engineering strategies capable of enhancing the structural and functional properties of aluminum has attracted sustained attention from both academia and industry.

Various surface modification techniques have been proposed to improve the performance of aluminum substrates, including anodization, thermal oxidation, sol–gel coatings, laser surface treatment, chemical conversion coatings, and plasma-assisted processes [5–8]. Among these approaches, plasma-based technologies have attracted considerable attention due to their ability to

* Corresponding authors.
*E-mail addresses:* dehghanyz93@gmail.com

**Cite this article as:**
Dehghani Z., 2027. Time-Dependent Growth Behavior of Alumina Layers on Aluminum during plasma-Assisted Electrochemical Oxidation in a Plasma–Liquid Interface. *Progress in Physics of Applied Materials*, *7*(1), pp.85-94.DOI: 10.22075/ppam.2026.41478.1236

generate highly reactive environments capable of inducing physicochemical transformations without requiring excessively high bulk temperatures [9]. The interaction of energetic electrons, ions, radicals, metastable species, and ultraviolet radiation with solid surfaces can substantially alter surface composition, morphology, crystallinity, and interfacial properties, thereby enabling the formation of functional oxide layers with tailored characteristics [10]. Recent studies have further demonstrated that plasma-based processes provide effective routes for fabricating functional oxide-containing surfaces and nanostructured materials through controlled plasma–surface interactions [11].

During the last decade, plasma–liquid interaction (PLI) systems have received growing attention as versatile platforms for materials processing, environmental remediation, biomedical applications, nanomaterial synthesis, and surface engineering [12–14]. In such systems, plasma is generated either within, above, or in direct contact with a liquid medium, leading to the formation of a highly reactive interface where physical and chemical processes occur simultaneously. The plasma–liquid interface is characterized by complex interactions involving energetic electrons, solvated electrons, reactive oxygen species (ROS), reactive nitrogen species (RNS), hydroxyl radicals, ionic species, and transient excited molecules [12,15]. These reactive species can initiate oxidation reactions, modify surface chemistry, and influence the nucleation and evolution of oxide layers on metallic substrates immersed in the electrolyte.

Among various plasma–liquid configurations, atmospheric-pressure microplasma systems have attracted increasing attention due to their operational simplicity, low power consumption, and ability to generate localized regions of high chemical reactivity [16,17]. Unlike conventional vacuum plasma technologies, atmospheric-pressure microplasmas eliminate the need for expensive vacuum infrastructure while maintaining non-equilibrium plasma characteristics [18]. Plasma-assisted fabrication strategies have also been explored for producing functional nanostructured surfaces, highlighting the capability of plasma systems for localized and controllable surface modification [19]. Furthermore, the small dimensions of microplasmas facilitate efficient energy transfer to the plasma–liquid interface and enable precise control over surface modification processes [20].

Recent investigations have demonstrated that microplasma-assisted electrochemical treatments can effectively modify the surfaces of various metallic materials, including titanium, magnesium, stainless steel, and aluminum [21–24]. In these systems, the simultaneous presence of electrochemical oxidation reactions and plasma-generated reactive species creates unique conditions that promote surface oxidation and oxide-layer development. Unlike conventional anodizing processes, plasma-assisted electrochemical oxidation introduces additional activation pathways through the continuous generation of chemically reactive species at the plasma–liquid interface [12, 25]. As a result, the structure and morphology of the resulting oxide layers can differ substantially from those obtained through purely electrochemical methods.

For aluminum substrates, plasma-assisted oxidation processes are particularly attractive because they can facilitate the formation of alumina-based surface layers with controlled surface morphology and crystalline structure. [26,27]. Aluminum oxide exists in several polymorphic forms, among which $\gamma$-$Al_2O_3$ is frequently observed under moderate processing conditions due to its relatively low formation energy and high surface area [28]. The formation of crystalline alumina coatings is of considerable interest because such layers can improve wear resistance, corrosion protection, adhesion behavior, and catalytic performance [29,30]. Previous studies have shown that the characteristics of alumina layers strongly depend on processing parameters such as electrolyte composition, gas atmosphere, applied electrical conditions, treatment duration, and reactor configuration [31–33].

Among these parameters, treatment time plays a particularly important role because it directly governs the duration of plasma exposure and consequently influences the cumulative interaction between reactive plasma species and the metallic surface [34]. During the initial stages of treatment, surface oxidation is expected to begin with localized oxide formation, followed by progressive surface evolution during prolonged plasma exposure. As treatment proceeds, continuous exposure to reactive oxygen-containing species promotes oxide growth and surface evolution. Simultaneously, prolonged plasma treatment may induce structural reorganization, densification, and phase development within the growing oxide layer [35]. Therefore, treatment duration can significantly affect surface roughness, microstructural organization, oxide crystallinity, and overall coating architecture.

Although plasma-assisted oxidation of aluminum has been investigated in several studies, most previous works have focused on discharge characteristics, plasma chemistry, corrosion behavior, or general coating formation mechanisms [22, 31, 12]. Comparatively, fewer studies have systematically examined the influence of treatment duration on the temporal evolution of alumina layers formed in atmospheric-pressure DC microplasma–liquid systems. In particular, the relationships between oxide nucleation, surface roughness evolution, morphological restructuring, and crystalline phase formation remain insufficiently understood. A comprehensive understanding of these processes is essential for establishing reliable processing–structure relationships and optimizing plasma-assisted surface engineering strategies.

In addition, many investigations reported in the literature have been conducted using plasma electrolytic oxidation (PEO) or micro-arc oxidation systems operating under substantially different discharge regimes [36–38]. In contrast, the present work employs an atmospheric-pressure DC microplasma generated above a NaOH electrolyte, where surface modification is primarily governed by plasma–liquid interactions, electrochemical oxidation reactions, and reactive-species-driven surface evolution. Consequently, the mechanisms controlling oxide

growth in the present configuration differ from those commonly associated with conventional PEO processes and require independent investigation.

Therefore, the objective of the present study is to elucidate the influence of treatment duration on the growth behavior of alumina layers formed on aluminum surfaces using a DC microplasma-assisted electrochemical process operating in a NaOH electrolyte under atmospheric-pressure conditions. Surface evolution was systematically investigated using atomic force microscopy (AFM), scanning electron microscopy (SEM), and X-ray diffraction (XRD) techniques. Particular attention was devoted to understanding the relationships among treatment duration, surface roughness evolution, morphological development, and phase formation. Based on the experimental observations, a growth mechanism describing the temporal evolution of the plasma-generated alumina layer is proposed. The findings provide new insights into plasma–liquid-assisted surface modification of aluminum and contribute to the development of controllable plasma-based oxidation processes for advanced engineering applications.

## 2. Materials and Methods

### *2.1. Materials*

Commercially pure aluminum sheets with a thickness of 1 mm were used as the substrate material in the present study. Prior to plasma treatment, the aluminum substrates were mechanically polished using successive grades of abrasive papers in order to obtain a relatively uniform surface condition. After polishing, the substrates were ultrasonically cleaned in distilled water and ethanol to remove residual contaminants and then dried in air before use. The electrolyte consisted of an aqueous sodium hydroxide (NaOH) solution prepared using analytical-grade NaOH and distilled water. The concentration of the electrolyte was maintained at 0.05 M throughout all experiments. Fresh electrolyte was prepared prior to each experimental run to ensure reproducibility of the plasma-assisted oxidation process.

In order to systematically evaluate the effect of treatment duration, all plasma operating parameters, including discharge current, electrode configuration, electrode spacing, and argon flow rate, were maintained constant during the experiments. This approach was selected to minimize the contribution of additional variables and to establish a direct relationship between plasma exposure time and the resulting surface evolution.

### *2.2. Plasma-in-liquid Reactor Configuration*

Microplasma treatment was carried out using a laboratory-scale plasma–liquid interaction reactor operating at atmospheric pressure. A schematic representation of the experimental setup is shown in Figure 1.

A DC high-voltage power supply was employed to generate a stable microplasma discharge above the electrolyte surface. A stainless-steel hollow needle was used as the cathode and positioned approximately 2 mm above the electrolyte surface. The aluminum specimen was immersed in the electrolyte and simultaneously served as the anode and the substrate subjected to surface modification.

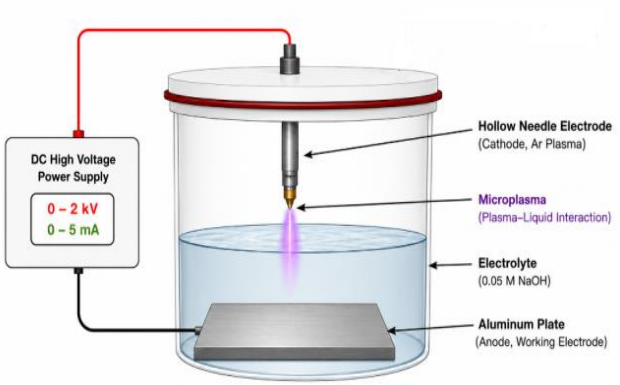


**Fig. 1.** A schematic representation of the experimental setup.

Argon gas was continuously introduced through the hollow cathode at a flow rate of 250 sccm in order to facilitate plasma ignition and maintain discharge stability. The plasma discharge was operated in constant-current mode at a discharge current of 5 mA. To suppress current fluctuations and stabilize the discharge, a ballast resistor of 100 kΩ was connected in series with the power supply. Voltage and current signals were continuously monitored during the experiments to ensure stable plasma operation. The interaction between the plasma discharge and the electrolyte generated a highly reactive environment containing energetic electrons, ions, ultraviolet radiation, hydroxyl radicals, oxygen-containing species, and other short-lived reactive intermediates. These species contributed to the oxidation and modification of the aluminum surface during treatment. The discharge voltage varied during plasma operation and reached values up to approximately 2 kV depending on the discharge conditions.

### *2.3. Microplasma-Assisted Surface Modification Procedure*

For each experiment, a fixed volume of NaOH electrolyte was poured into a glass reactor. The aluminum substrate was vertically immersed in the electrolyte at a constant position to ensure identical discharge geometry and plasma exposure conditions throughout all experiments. Following stabilization of the argon flow, the plasma discharge was ignited above the electrolyte surface and maintained for different treatment durations of 5, 10, and 20 min. During plasma exposure, the energetic species generated within the plasma–liquid interface interacted with the aluminum substrate and promoted electrochemical oxidation reactions. Simultaneously, plasma exposure provided additional chemical and interfacial activation through reactive species generation and localized energy transfer, thereby promoting oxidation and surface modification.

To evaluate the influence of treatment duration on coating evolution, all operating parameters including gas flow rate, discharge current, electrode configuration, electrode spacing, and electrolyte composition were kept constant. Therefore, treatment time was considered the

primary experimental variable governing the development of surface morphology and phase composition.

The selected treatment durations (5, 10, and 20 min) were chosen to represent different stages of surface evolution under plasma-assisted oxidation conditions. The shortest treatment time was selected to investigate the initial surface modification, while intermediate and prolonged treatment times were considered to evaluate the development and restructuring of the oxide layer during extended plasma exposure. These conditions allowed the temporal evolution of surface morphology and structural changes to be systematically compared.

### *2.4. Characterization Techniques*

The surface morphology of the plasma-treated aluminum samples was examined using scanning electron microscopy (SEM). SEM observations were performed to evaluate morphological evolution, pore formation, and the development of surface microstructures after plasma treatment.

Surface topography and roughness characteristics were investigated using atomic force microscopy (AFM). AFM measurements were performed in non-contact mode to minimize tip-induced surface deformation during scanning. Three-dimensional topographical images were analyzed to obtain quantitative surface roughness parameters, including the arithmetic average roughness (Ra), root mean square roughness (Rq), and maximum height variation (Rt). All measurements were conducted using identical instrumental settings and analysis procedures to ensure consistent comparison among samples treated under different plasma exposure times.

The crystalline structure and phase composition of the modified surfaces were analyzed by X-ray diffraction (XRD) using Cu Kα radiation (λ = 1.5406 Å). Diffraction patterns were recorded over an appropriate 2θ range to identify the phases formed during plasma-assisted oxidation. The obtained diffraction peaks were compared with standard reference data to determine the presence of crystalline alumina phases and residual aluminum substrate peaks.

To improve the reliability of the results, all measurements were performed under identical experimental conditions, and the obtained data were analyzed comparatively as a function of plasma treatment duration.

## 3. Results and Discussion

### *3.1. XRD Analysis*

The phase composition of the aluminum surface after microplasma-assisted electrochemical treatment was investigated by XRD, and the corresponding diffraction pattern is presented in Fig. 2. As can be observed, the diffraction pattern consists of characteristic reflections associated with both the aluminum substrate and the oxide layer formed during plasma treatment. The detected $\gamma$-$Al_2O_3$ reflections reveal presence of crystalline $\gamma$-$Al_2O_3$ in the oxide layer formed after 20 min of treatment.

The diffraction peaks observed at approximately 45-46° and 66-67° were assigned to the (200) and (220) crystallographic planes of metallic aluminum, respectively. The presence of these peaks indicates that the X-ray beam partially penetrated through the oxide layer and interacted with the underlying aluminum substrate. This observation suggests that the oxide coating thickness remained within the effective penetration depth of the incident X-rays, allowing substrate reflections to remain visible in the diffraction pattern.

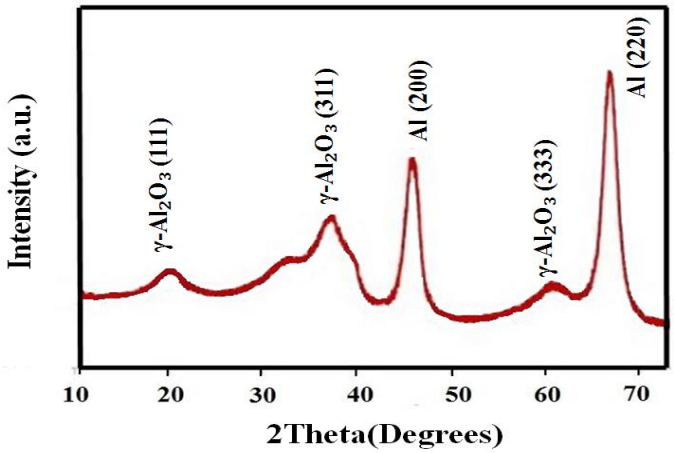


**Fig. 2.** XRD spectrum of the aluminum specimen treated by the DC microplasma-assisted electrochemical process for 20 min.

In addition to the aluminum peaks, several diffraction signals corresponding to $\gamma$-$Al_2O_3$ were detected. Characteristic reflections indexed to the (111), (311), and (333) planes of $\gamma$-$Al_2O_3$ were observed at approximately 20°, 37°, and 61°, respectively. The appearance of these peaks confirms the formation of crystalline alumina during the microplasma-assisted oxidation process.

The formation of $\gamma$-$Al_2O_3$ may be associated with the combined effects of plasma-generated oxygen-containing species, electrochemical oxidation reactions, and localized energy transfer occurring at the plasma–liquid interface. During plasma operation, energetic electrons, ions, and reactive oxygen-containing species interact with the aluminum surface, resulting in rapid oxidation and oxide growth. Similar $\gamma$-$Al_2O_3$ formation has been reported in plasma-assisted oxidation systems and plasma–liquid interaction environments [39].

The predominance of $\gamma$-$Al_2O_3$ rather than $\alpha$-$Al_2O_3$ is consistent with the relatively short treatment duration and moderate discharge current employed in the present work. According to previous investigations [39,40], $\gamma$-$Al_2O_3$ is generally considered a metastable phase that forms during the early and intermediate stages of plasma-assisted oxidation, whereas the formation of thermodynamically stable $\alpha$-$Al_2O_3$ typically requires higher discharge energies, prolonged treatment times, or more severe thermal conditions.

Furthermore, the relatively broad nature of the $\gamma$-$Al_2O_3$ diffraction peaks suggests that the oxide layer may consist of fine crystalline domains together with partially amorphous regions. The relatively broad diffraction peaks may indicate the coexistence of fine crystalline domains

and partially disordered oxide regions. The coexistence of crystalline γ-$Al_2O_3$ and residual aluminum substrate peaks therefore indicates the successful formation of a plasma-induced oxide layer while preserving the structural integrity of the metallic substrate.

Overall, the XRD results demonstrate that the DC microplasma-assisted electrochemical process effectively promoted the oxidation of aluminum and led to the formation of crystalline γ-$Al_2O_3$ on the treated surface. The presence of this phase is expected to contribute significantly to the modification of surface properties and is consistent with the morphological evolution observed in the AFM and SEM analyses discussed in the following sections.

### *3.2. AFM Analysis*

Atomic force microscopy (AFM) was employed to investigate the influence of microplasma treatment time on the evolution of surface topography and roughness of the aluminum substrate. Three-dimensional AFM images of the treated samples are presented in Figure 3, while the corresponding roughness parameters are summarized in Table 1.

**Table 1.** Surface roughness parameters obtained from AFM measurements for aluminum samples treated by the DC microplasma-assisted electrochemical process at different treatment times.

| Treatment time (min) | Ra (nm) | Rq (nm) | Rt (nm) |
|---|---|---|---|
| 5 | 114.44 | 161.14 | 1546.83 |
| 10 | 174.33 | 209.48 | 1174.85 |
| 20 | 80.25 | 105.43 | 718.87 |

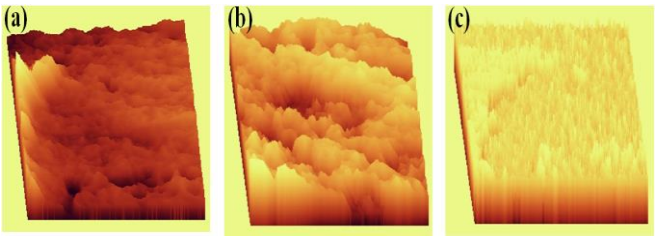


**Fig. 3.** Three-dimensional AFM topography images of aluminum surfaces treated by the DC microplasma-assisted electrochemical process for different treatment durations: (a) 5 min, (b) 10 min, and (c) 20 min.

Considering the above figure, the evolution of surface roughness and topographical features indicates progressive oxide growth and plasma-induced surface restructuring.

Following plasma treatment, substantial modifications in the surface topography were observed, indicating that the plasma–liquid interaction significantly affected the oxidation behavior and surface growth mechanism. For the sample treated for 5 min, the surface displayed the initial stages of oxide formation accompanied by the development of localized protrusions and nanoscale surface irregularities. The average roughness (Ra) and root-mean-square roughness (Rq) were measured to be 114.44 nm and 161.14 nm, respectively. These values suggest that oxide nucleation had already occurred across the surface, leading to a noticeable increase in topographical heterogeneity.

Increasing the treatment duration to 10 min resulted in a pronounced modification of the surface morphology. The roughness parameters increased significantly, reaching Ra and Rq values of 174.33 nm and 209.48 nm, respectively. This increase indicates enhanced oxide growth and a higher density of discharge-induced surface features. The elevated roughness can be attributed to the intensified microplasma activity occurring at the plasma–electrolyte interface, which promoted localized oxidation, material redistribution, and the formation of larger surface asperities. At this stage, the competition between oxide growth and plasma-induced restructuring appears to favor rapid topographical development, resulting in the highest roughness values observed among the investigated samples.

Interestingly, further increasing the treatment time to 20 min led to a reduction in roughness, with Ra and Rq decreasing to 80.25 nm and 105.43 nm, respectively. A similar trend was observed for the maximum height variation (Rt), which decreased from 1546.83 nm at 5 min and 1174.85 nm at 10 min to 718.87 nm after 20 min of treatment. This behavior suggests that prolonged plasma exposure induced a surface reorganization process. Repeated plasma exposure and continuous interaction with reactive species may promote surface reorganization and partial smoothing of previously formed asperities.

The observed roughness evolution reveals that surface development during the microplasma-assisted process does not follow a simple monotonic trend. Instead, the process involves two competing mechanisms: continuous oxide growth, which tends to increase roughness, and plasma-induced surface restructuring, which may reduce large height fluctuations during prolonged treatment. Similar non-monotonic roughness evolution has been reported in plasma-assisted and plasma–liquid surface modification systems, where oxide growth and surface reorganization may occur concurrently. The AFM observations therefore suggest that treatment duration plays a critical role in determining the final surface architecture of the plasma-modified aluminum. During the early stages of treatment, oxide nucleation and discharge-induced growth dominate the process, leading to increasing roughness. At longer treatment times, however, discharge-driven restructuring mechanisms become increasingly significant, resulting in a more uniform topography despite the continued development of the oxide layer.

Overall, the AFM results demonstrate that the microplasma-assisted electrochemical treatment effectively alters the nanoscale surface characteristics of aluminum. The temporal evolution of roughness observed in the present study provides valuable insight into the dynamic growth behavior of plasma-induced alumina

layers and supports the phase formation results obtained from XRD analysis.

### *3.3. SEM Analysis*

The surface morphology of the aluminum specimen treated for 20 min was investigated using scanning electron microscope (SEM), and the corresponding micrographs are presented in Figure 4. As shown in the figure, the treated surface exhibits a highly developed three-dimensional morphology consisting of interconnected needle-like structures distributed over the substrate and porous morphological features formed as a result of plasma-induced oxidation and surface restructuring. The formation of such features indicates that the DC microplasma-assisted electrochemical treatment significantly altered the surface architecture of the aluminum substrate.

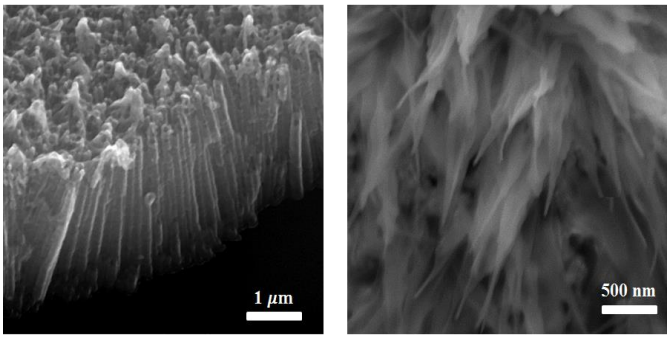


**Fig. 4.** SEM micrograph of the aluminum surface after 20 min of DC microplasma-assisted electrochemical treatment in 0.05 M NaOH electrolyte.

Compared with the relatively smooth morphology expected for the polished aluminum surface, the treated specimen displays a considerably more complex topography characterized by elongated oxide features, localized agglomerates, and porous regions. These observations confirm that prolonged exposure to the plasma–liquid environment promoted substantial surface modification and oxide-layer development.

The observed needle-like morphology suggests that oxide growth did not occur uniformly across the entire surface. Instead, surface evolution appears to have been governed by localized plasma–surface interactions and the continuous availability of reactive species generated at the plasma–liquid interface. Under such conditions, preferential growth may occur at specific surface sites, leading to the gradual development of vertically oriented oxide structures and an increasingly heterogeneous surface morphology.

Another notable characteristic of the treated surface is the presence of porous features distributed throughout the oxide layer. The formation of pores is commonly observed in plasma-assisted oxidation systems and may be associated with the combined effects of interfacial reactions, gas evolution, and non-uniform oxide growth during treatment. The coexistence of porous regions and elongated oxide structures indicates that multiple surface-evolution processes occurred simultaneously throughout the treatment period.

The SEM observations also provide valuable insight into the structural evolution of the oxide layer when considered together with the AFM results. Although the roughness values obtained from AFM decreased after prolonged treatment, the SEM micrographs reveal the formation of more organized and interconnected surface structures. This observation suggests that extended plasma exposure promoted structural reorganization of the growing oxide layer rather than a simple increase in surface roughness. Consequently, the reduction in roughness observed after 20 min does not necessarily indicate reduced oxide formation, but rather reflects a change in the mode of surface development.

Furthermore, the interconnected nature of the observed structures suggests progressive growth and integration of neighboring oxide domains during treatment. As the oxide layer continued to develop, individual surface features gradually became linked, resulting in a more continuous and structurally coherent morphology. Such behavior is consistent with the evolution expected in plasma-assisted electrochemical oxidation processes, where continuous interaction between reactive species and the substrate promotes ongoing oxide formation and surface restructuring.

The SEM observations are also in agreement with the XRD results, which confirm the presence of crystalline γ-$Al_2O_3$ on the treated surface. The coexistence of crystalline alumina and a highly developed oxide morphology indicates that the plasma-assisted treatment not only modified the chemical composition of the surface but also substantially influenced its microstructural organization.

Overall, the SEM investigation demonstrates that prolonged DC microplasma-assisted electrochemical treatment leads to the formation of a porous alumina layer composed of interconnected needle-like structures. The observed morphology reflects the cumulative effects of plasma–liquid interactions, reactive-species-driven oxidation, and progressive surface reorganization during treatment.

The AFM, SEM, and XRD results provide complementary information regarding the evolution of the plasma-treated aluminum surface. AFM analysis reveals nanoscale roughness changes during different treatment durations, SEM demonstrates the development of microstructural features, while XRD provides evidence of crystalline phase formation. The combined analysis suggests that plasma exposure induces simultaneous oxidation, morphological development, and structural organization of the surface layer.

### *3.4. Proposed Growth Mechanism*

Based on the combined observations obtained from XRD, AFM, and SEM analyses, a growth mechanism is proposed to describe the temporal evolution of the

alumina layer formed on the aluminum surface during DC microplasma-assisted electrochemical treatment. The mechanism is schematically illustrated in Figure 5 and consists of three successive stages corresponding to the investigated treatment durations. It should be noted that the proposed mechanism is derived from the observed morphological and structural evolution of the surface and is interpreted in the context of plasma–liquid interaction phenomena occurring at the plasma–electrolyte interface.

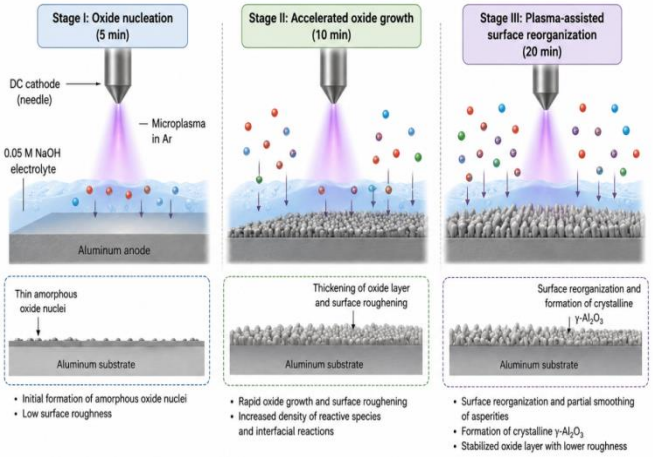


**Fig. 5.** Proposed three-stage growth mechanism of the alumina layer formed on aluminum during DC microplasma-assisted electrochemical oxidation in a plasma–liquid system: (I) nucleation of discrete alumina islands on the aluminum surface, (II) progressive oxide growth and surface roughening promoted by continuous interaction with plasma-generated reactive species, and (III) surface reorganization accompanied by the formation of crystalline γ-$Al_2O_3$ and interconnected needle-like oxide structures.

*Stage I: Initial Oxide Nucleation (0–5 min)*

At the beginning of the treatment process, plasma generation above the electrolyte surface produces a reactive environment containing energetic electrons, excited argon species, hydroxyl radicals, oxygen-containing reactive species, and ionic intermediates. These species continuously interact with the electrolyte and the aluminum substrate, promoting electrochemical oxidation reactions at the metal–electrolyte interface.

During this stage, oxidation occurs primarily through the formation of discrete oxide nuclei distributed across the aluminum surface. The AFM results obtained after 5 min of treatment indicate the emergence of localized surface irregularities and a noticeable increase in surface heterogeneity compared with the polished substrate. These observations suggest that the surface modification process is initially governed by oxide nucleation and localized growth rather than by the development of a continuous thick oxide layer.

Consequently, the surface at this stage can be described as a partially covered aluminum substrate containing isolated alumina nuclei and relatively limited topographical development.

*Stage II: Accelerated Oxide Growth and Surface Roughening (5–10 min)*

With increasing treatment duration, continuous exposure to reactive plasma-generated species enhances oxidation kinetics and promotes the growth of previously formed oxide nuclei. As neighboring nuclei expand, the oxide layer progressively develops both laterally and vertically, resulting in a more complex surface architecture.

The AFM measurements revealed that the highest roughness values were obtained after 10 min of treatment. This increase in roughness indicates that oxide growth becomes the dominant process during this period. The enhanced interaction between reactive species and the substrate surface facilitates the accumulation of oxidation products and contributes to the formation of pronounced surface asperities.

The observed roughening behavior suggests that the oxide layer undergoes rapid development during this stage, leading to the formation of a highly heterogeneous surface characterized by significant height variations. Therefore, Stage II may be regarded as the principal oxide-growth regime within the investigated treatment window.

*Stage III: Surface Reorganization and Formation of Crystalline Alumina (10–20 min)*

Further extension of the treatment duration results in a noticeable change in surface evolution behavior. Although oxidation continues to occur, the AFM data demonstrate a reduction in roughness after 20 min of treatment. Simultaneously, SEM observations reveal the formation of more organized and interconnected oxide structures distributed across the surface.

This behavior suggests that prolonged plasma exposure promotes surface reorganization in addition to continued oxide growth. As the oxide layer becomes more developed, localized growth processes gradually lead to the formation of a more continuous and structurally integrated surface morphology. The reduction in roughness observed by AFM indicates that large-scale height fluctuations become less pronounced despite the continued development of oxide structures at the microscale.

XRD analysis further revealed the presence of crystalline γ-$Al_2O_3$ on the treated surface. The appearance of this phase indicates that the plasma-assisted electrochemical environment provides conditions favorable for the formation of crystalline alumina during extended treatment. The coexistence of crystalline γ-$Al_2O_3$ together with the interconnected needle-like morphology observed by SEM suggests that structural organization and phase development occur simultaneously during this stage.

*Overall Growth Behavior*

The overall evolution of the alumina layer appears to be governed by the interplay between two concurrent processes: oxide growth and surface reorganization. During the early stages of treatment, oxide nucleation and subsequent growth dominate the surface evolution,

resulting in a progressive increase in roughness. As treatment proceeds, however, continued plasma exposure promotes structural reorganization of the growing oxide layer, leading to a more integrated surface morphology and a reduction in large-scale roughness features.

Accordingly, the temporal evolution observed in the present study can be summarized as a sequence of oxide nucleation, accelerated oxide growth, and plasma-assisted surface reorganization accompanied by the formation of crystalline γ-$Al_2O_3$. This mechanism provides a consistent interpretation of the AFM, SEM, and XRD results and highlights the critical role of treatment duration in controlling the structural development of alumina layers formed in plasma–liquid interaction systems.

The NaOH electrolyte plays a dual role in the plasma-assisted oxidation process. First, it provides sufficient ionic conductivity for electrochemical reactions between the aluminum substrate and the electrolyte. Second, the alkaline environment facilitates interfacial reactions involving oxygen-containing species generated during plasma–liquid interaction, contributing to oxide formation and surface modification.

It should be emphasized that the proposed three-stage mechanism represents a possible interpretation of the observed morphological and structural evolution rather than a direct observation of individual oxidation steps. The mechanism is proposed based on the correlation between surface roughness variation, morphological characteristics, and phase evolution obtained from AFM, SEM, and XRD analyses.

## 4. Conclusions

In this study, aluminum surfaces were successfully modified using a DC microplasma-assisted electrochemical process operated in a 0.05 M NaOH electrolyte under atmospheric-pressure conditions. The influence of treatment duration on the evolution of surface morphology, roughness, and phase composition was systematically investigated using AFM, SEM, and XRD analyses.

The obtained results demonstrated that treatment time strongly affected the development of the oxide layer. AFM measurements revealed that surface roughness increased during the initial stages of treatment and reached a maximum value after 10 min, indicating enhanced oxide growth and topographical evolution. Further extension of the treatment duration led to a reduction in roughness, suggesting the occurrence of plasma-assisted surface reorganization processes.

XRD analysis indicated the formation of a γ-$Al_2O_3$-related crystalline phase based on the characteristic diffraction reflections observed in the treated sample. Although XRD provides valuable information regarding phase development, the identification of thin oxide layers on aluminum substrates may be affected by substrate diffraction contributions. Therefore, the observed γ-$Al_2O_3$ formation should be considered as an indication of crystalline alumina development under the applied plasma-assisted oxidation conditions.

By correlating the XRD, AFM, and SEM results, a growth mechanism consisting of three sequential stages was proposed: (i) initial oxide nucleation, (ii) rapid oxide growth accompanied by roughness increase, and (iii) plasma-induced restructuring and crystallization of the oxide layer. The results indicate that treatment duration is a key processing parameter governing the structural evolution of microplasma-generated alumina coatings.

Overall, the present findings demonstrate that DC microplasma-assisted electrochemical treatment provides an effective approach for producing alumina-containing surface layers with controllable surface characteristics on aluminum substrates. The present results improve the understanding of the time-dependent surface evolution occurring during plasma-assisted electrochemical oxidation and highlight the potential of this technique for controlled surface modification of aluminum under atmospheric-pressure conditions.

## Funding Statement

This research received no specific grant from any funding agency.

## Conflicts of Interest

The author declares that there are no known competing financial interests or personal relationships that could have appeared to influence the work reported in this paper.

## Authors Contribution Statement

The author solely contributed to all aspects of this work, including conceptualization, methodology, analysis, and manuscript preparation.

## References

[1] Davis, J.R. (Ed.). 1999. Corrosion of aluminum and aluminum alloys. Asm International.

[2] Totten, G.E., & MacKenzie, D.S. (Eds.). 2003. Handbook of aluminum: vol. 1: physical metallurgy and processes. CRC press.

[3] Brandt, J.L., Frank, W.B., Koch, G.P., Mills, J.J., & Hatch, J.E. 1984. Aluminum Properties and Physical Metallurgy. American Society for Metals, 1.

[4] Polmear, I.J. 2005. Light Alloys. Butterworth-Heinemann.

[5] Diggle, J.W., Downie, T.C., & Goulding, C.W. 1969. Anodic oxide films on aluminum. *Chemical Reviews*, 69(3), pp.365-405.

[6] Fernández López, P. 2023. Plasma electrolytic oxidation technology for the development of high-performance coatings on cast Al-Si alloys. Doctoral

dissertation, Universidad del País Vasco-Euskal Herriko Unibertsitatea.

[7] Thompson, G.E. 1997. Porous anodic alumina: fabrication, characterization and applications. *Thin solid films*, 297(1-2), pp.192-201.

[8] Wang, D., & Bierwagen, G.P. 2009. Sol–gel coatings on metals for corrosion protection. Progress in organic coatings, 64(4), pp.327-338.

[9] Tendero, C., Tixier, C., Tristant, P., Desmaison, J., & Leprince, P. 2006. Atmospheric pressure plasmas: A review. *Spectrochimica Acta Part B: Atomic Spectroscopy*, 61(1), pp.2-30.

[10] Fridman, A. 2008. Plasma chemistry. Cambridge university press.

[11] Kiamehr, Z. 2025. Preparation of TiO2 Nanostructures and Its Plasma Coating in the Dye-Sensitized Solar Cell. *Progress in Physics of Applied Materials*, 5(1), pp.11-16.

[12] Bruggeman, P.J., Kushner, M.J., Locke, B.R., Gardeniers, J.G., Graham, W.G., Graves, D.B., ... & Zvereva, G. 2016. Plasma–liquid interactions: a review and roadmap. *Plasma sources science and technology*, 25(5), pp.053002.

[13] Mariotti, D., Patel, J., Švrček, V., & Maguire, P. 2012. Plasma–liquid interactions at atmospheric pressure for nanomaterials synthesis and surface engineering. *Plasma Processes and Polymers*, 9(11-12), pp.1074-1085.

[14] Bruggeman, P., & Leys, C. 2009. Non-thermal plasmas in and in contact with liquids. *Journal of Physics D: Applied Physics*, 42(5), pp.053001.

[15] Lukes, P., Locke, B.R., & Brisset, J.L. 2012. Aqueous-phase chemistry of electrical discharge plasma in water and in gas-liquid environments. *Plasma chemistry and catalysis in gases and liquids*, 1, pp.243-308.

[16] Mariotti, D., & Sankaran, R.M. 2010. Microplasmas for nanomaterials synthesis. Journal of Physics D: Applied Physics, 43(32), pp.323001.

[17] Becker, K.H., Schoenbach, K.H., & Eden, J.G. 2006. Microplasmas and applications. *Journal of Physics D: Applied Physics*, 39(3), pp.R55-R70.

[18] Schoenbach, K.H., & Becker, K. 2016. 20 years of microplasma research: a status report. *The European Physical Journal D*, 70(2), pp.29.

[19] Abedi Jondani, M.R., Shariat, M., & Sadeghzadeh Lari, E. 2025. Recyclable Ag-$TiO_2$ SERS Substrates Fabricated via Plasma Jet Printing. *Progress in Physics of Applied Materials*, 5(2), pp.117-123.

[20] Eden, J.G., Park, S.J., Cho, J.H., Kim, M.H., Houlahan, T.J., Li, B., Kim, E.S., Kim, T.L., Lee, S.K., Kim, K.S., & Yoon, J.K. 2013. Plasma science and technology in the limit of the small: Microcavity plasmas and emerging applications. *IEEE Transactions on Plasma Science*, 41(4), pp.661-675.

[21] Reuter, S., & Hamdan, A. 2025. Plasma and Liquids—Fundamentals and Applications. Plasma Processes & Polymers, 22(1).

[22] Patel, V.K., & Bhowmik, S. 2017. Plasma processing of aluminum alloys to promote adhesion: A critical review. *Reviews of Adhesion and Adhesives*, 5(1), pp.79-104.

[23] Lu, X., Reuter, S., Laroussi, M., & Liu, D. 2019. Nonequilibrium atmospheric pressure plasma jets: Fundamentals, diagnostics, and medical applications. CRC Press.

[24] Kim, M.C., Yang, S.H., Boo, J.H., & Han, J.G. 2003. Surface treatment of metals using an atmospheric pressure plasma jet and their surface characteristics. *Surface and coatings Technology*, 174, pp.839-844.

[25] Bruggeman, P.J., Iza, F., & Brandenburg, R. 2017. Foundations of atmospheric pressure non-equilibrium plasmas. *Plasma Sources Science and Technology*, 26(12), pp.123002.

[26] Lee, W., & Park, S.J. 2014. Porous anodic aluminum oxide: anodization and templated synthesis of functional nanostructures. *Chemical reviews*, 114(15), pp.7487-7556.

[27] McCafferty, E. 2010. Introduction to corrosion science. Springer Science & Business Media.

[28] Levin, I., & Brandon, D. 1998. Metastable alumina polymorphs: crystal structures and transition sequences. *Journal of the american ceramic society*, 81(8), pp.1995-2012.

[29] Letyagin, N.V., Akopyan, T.K., Sokorev, A.A., Sviridova, T.A., Cherkasov, S.O., & Mansurov, Y.N. 2023. The characterization of coatings formed on as-cast Al, Al–Si, and Al–Ca aluminum substrates by plasma electrolytic oxidation. *Metals*, 13(9), pp.1509.

[30] Paglia, G., Buckley, C.E., Rohl, A.L., Hart, R.D., Winter, K., Studer, A.J., ... & Hanna, J.V. 2004. Boehmite derived γ-alumina system. 1. Structural evolution with temperature, with the identification and structural determination of a new transition phase, γ '-alumina. *Chemistry of materials*, 16(2), pp.220-236.

[31] Hussein, R.O. 2015. Plasma Process Control for Improved PEO Coatings on Magnesium Alloys.

[32] Rogov, A.B., Yerokhin, A., & Matthews, A. 2018. The role of cathodic current in plasma electrolytic oxidation of aluminium: current density 'scanning waves' on complex-shape substrates. *Journal of Physics D: Applied Physics*, 51(40), pp.405303.

[33] Curran, J.A., & Clyne, T.W. 2005. Thermo-physical properties of plasma electrolytic oxide coatings on aluminium. *Surface and Coatings Technology*, 199(2-3), pp.168-176.

[34] Zhu, M., Song, Y., Dong, K., Shan, D., & Han, E.H. 2022. Effect of initial oxide film on the formation and performance of plasma electrolytic oxidation coating on 7075 aluminum alloy. *Acta Metallurgica Sinica (English Letters)*, 35(9), pp.1559-1571.

[35] Tsai, D.S., & Chou, C.C. 2021. Influences of growth species and inclusions on the current–voltage behavior of plasma electrolytic oxidation: A review. *Coatings*, 11(3), pp.270.

[36] Yerokhin, A.L., Nie, X., Leyland, A., Matthews, A., & Dowey, S.J. 1999. Plasma electrolysis for surface engineering. Surface and coatings technology, 122(2-3), pp.73-93.

[37] Hussein, R.O., Northwood, D.O., & Nie, X. 2013. The effect of processing parameters and substrate composition on the corrosion resistance of plasma electrolytic oxidation (PEO) coated magnesium alloys. *Surface and Coatings Technology*, 237, pp.357-368.

[38] Matykina, E., Arrabal, R., Mohamed, A., Skeldon, P., & Thompson, G.E. 2009. Plasma electrolytic oxidation of pre-anodized aluminium. *Corrosion Science*, 51(12), pp.2897-2905.

[39] Dehnavi, V., Liu, X.Y., Luan, B.L., Shoesmith, D.W., & Rohani, S. 2014. Phase transformation in plasma electrolytic oxidation coatings on 6061 aluminum alloy. *Surface and Coatings Technology*, 251, pp.106-114.

[40] Bousser, E., Rogov, A., Shashkov, P., Gholinia, A., Laugel, N., Slater, T.J., Withers, P.J., Matthews, A., & Yerokhin, A. 2023. Phase transitions in alumina films during post-sparking anodising of Al alloys. *Acta Materialia*, 244, pp.118587.